Five-degree-of-freedom active magnetic bearing with homopolar magnetic fields

Satoshi UENO*, Kazuma YAMAUCHI* and Changan ZHOA*
* Department of Mechanical Engineering, College of Science and Engineering, Ritsumeikan University
1-1-1 Nojihigashi, Kusatsu, Shiga 525-8577, Japan
E-mail: sueno@se.ritsumei.ac.jp

Abstract
This paper introduces a novel five-degree-of-freedom actively controlled magnetic bearing that combines an axial active magnetic bearing with radial force and tilting torque control functions. Attaching bias permanent magnets to the rotor and generating both homopolar and bipolar magnetic fields in the stator enables active control of the axial and radial forces and tilting torque with low power consumption and minimal rotating loss. The results of levitation tests shows that the proposed bearing is capable of five-axis active control.

Keywords : Active magnetic bearing, 5-DOF active control, homopolar magnetic fields, low-loss AMB

1. Introduction

Currently, there is a growing demand for wind power as a renewable energy source. Wind turbines can be broadly classified into two types: horizontal-axis wind turbines and vertical-axis wind turbines (VAWTs). VATs can generate electricity at relatively low wind speeds and do not require a specific wind direction, making them ideal for areas with unstable wind patterns (Mahmoud et al., 2020). Since these turbines are expected to be installed in large numbers, it is appropriate to use magnetic bearings to reduce the frequency of maintenance.

Magnetic bearings have many advantages, such as contamination-, lubrication-, and maintenance-free. However, their large size is one of the disadvantages. To overcome this, combined magnetic bearings have been developed such as the three-degree-of-freedom (DOF) control type active magnetic bearing (AMB) (Chen and Lin, 2016, Matsuzaki et al., 2016, Nakajima et al., 2018), which combines with an axial AMB and a radial AMB, and the self-bearing motor (Ueno et al., 2022), which combines a motor and radial or axial AMBs. Another disadvantage is a power consumption; permanent magnets are often used in magnetic bearings to reduce it. However, a heteropolar magnetic field in the air gap increases rotational loss. Therefore, a homopolar magnetic field is suitable for reducing both power consumption and rotational loss.

This paper introduces a novel five-DOF actively controlled magnetic bearing. The proposed AMB combines an axial AMB with radial force and tilting torque control functions. Using a homopolar bias permanent magnetic field and bipolar magnetic fields generated by the stator current allows for active control of the axial force, radial force, and tilting torque. This paper presents the structure and principle of the proposed AMB, as well as the results of levitation tests.

2. Structure and principles

2.1. Structure

The structure of the proposed AMB is shown in Fig. 1. The middle part is a stator, and the upper and lower parts are a rotor. In an actual device, the upper and lower rotors are fixed together as a unit. A ring permanent magnet (PM) magnetized in the thickness direction is attached to the rotor, and a homopolar magnetic field is generated in the air gap. A cylindrical magnetic path is attached to the outside of the rotors and stator to form a magnetic circuit. The PM flux passes through the rotor core, the outer cylinder, and the stator core, and returns to the PM. The stator coils generate homopolar and bipolar magnetic fields. In Fig. 1, the coils are air cores, but they can also be iron cores.

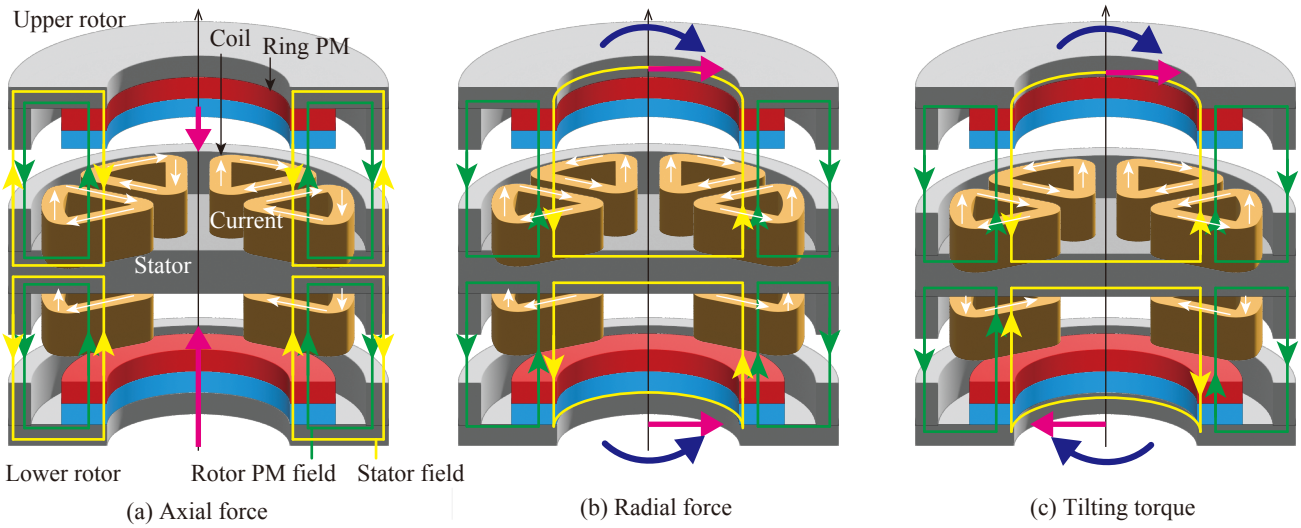

Fig. 1 The structure of a five-DOF AMB, and the generation of the axial force, radial force, and tilting torque.

2.2. Principles

Figure 1(a) shows the axial force generation. The white, yellow, and green lines represent the coil currents, the magnetic fields generated by the stator coils, and the magnetic fields generated by the rotor PMs, respectively. By generating the homopolar magnetic field in the opposite direction to the rotor PM at the top and in the same direction at the bottom, the upward axial force is obtained.

Figure 1(b) and (c) show the generation of radial force and tilting torque. The stator coils generate bipolar magnetic fields, and these fields do not pass through the cylindrical path. The magnetic field at the air gap is unbalanced by the bipolar fields, and the tilting torque is obtained. In addition, since the coil currents generate the Lorentz force, the radial force is obtained. By changing the direction of the coil currents at the top and bottom, the tilting torque or radial force is canceled, and then the they can be controlled independently. Although the radial force is also generates the tilting torque because the center of the gravity is not in the same position to the force, this torque enhances the tilting torque, so it does not become a problem.

2.3. Suspension force

Figure 2 shows the coordinate system. For simplicity, the magnetic resistance of the iron core and the leakage magnetic flux are neglected. The PM is considered divided into six pieces, with each piece as forming an independent magnetic circuit. The air gap at each coil is given by the following equations:

$$g_{u,k} = g_0 + z + r_p \sin\frac{(2k-1)\pi}{6}\theta_x - r_p \cos\frac{2(k-1)\pi}{6}\theta_y \tag{1}$$

$$g_{l,k} = g_0 - z - r_p \sin\frac{(2k-1)\pi}{6}\theta_x + r_p \cos\frac{2(k-1)\pi}{6}\theta_y \tag{2}$$

where g_0 is the air gap at the equilibrium position, z, θ_x, θ_y are displacement, r_p is average radius of the PM, k is the number of the coil ($k = 1 \sim 6$). The magnetic flux densities are calculated as

$$B_{s,k} = \frac{H_c t_p + N i_{s,k}}{R_{s,k}} \frac{1}{A_p/6} = \frac{\mu_0 (H_c t_p + N i_{s,k})}{2g_{s,k} + t_p + t_c} \tag{3}$$

where $R_{s,k}$ is magnetic resistance, H_c is coercivity of the PM, t_p and t_c is thickness of the PM and the coils, A_p is the area of the PM, μ_0 is permeability of the air, s is the index of the stator (u or l), N is the turn number of the coil, and $i_{s,k}$ is the coil current. The currents are defined as

$$i_{u,k} = -i_z + \left(-i_{\theta x} - i_y\right)\sin\frac{(2k-1)\pi}{6} + \left(i_{\theta y} - i_x\right)\cos\frac{(2k-1)\pi}{6} \tag{4}$$

$$i_{l,k} = i_z + \left(i_{\theta x} - i_y\right)\sin\frac{(2k-1)\pi}{6} + \left(-i_{\theta y} - i_x\right)\cos\frac{(2k-1)\pi}{6} \tag{5}$$

where $i_z, i_x, i_y, i_{\theta x}$, and $i_{\theta y}$ are control currents. The magnetic attractive force at each coil is expressed by

$$f_{s,k} = \frac{A_c (B_b + B_{c,s,k})^2}{2\mu_0} \tag{6}$$

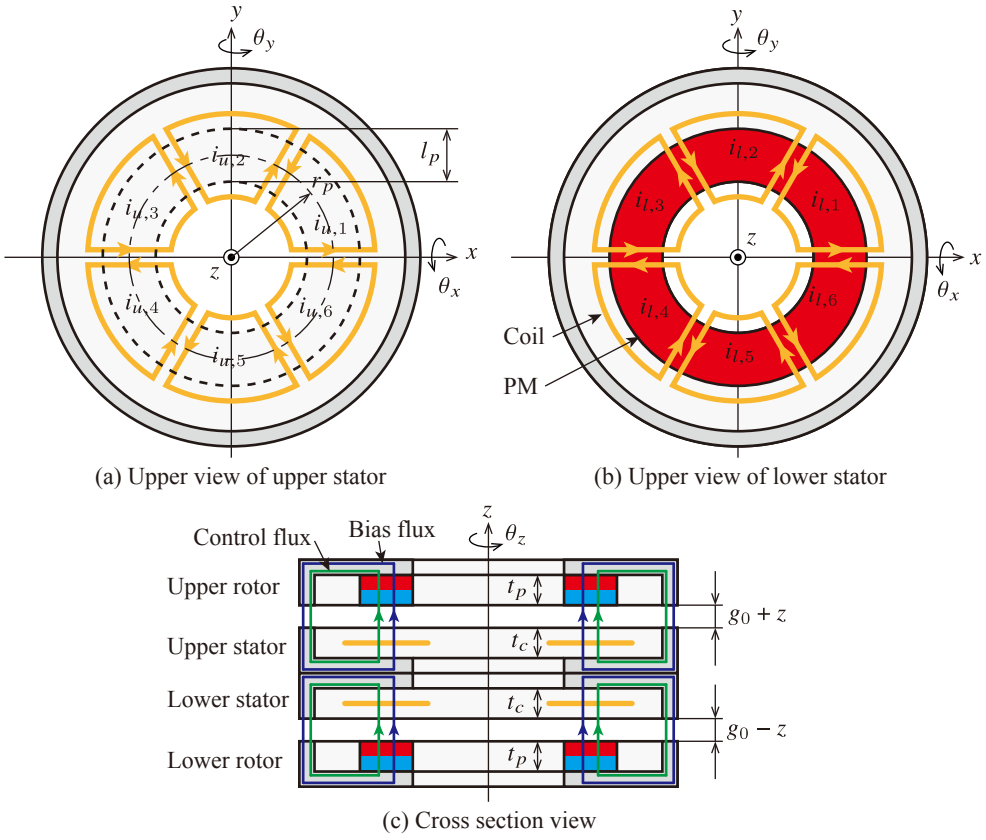

(a) Upper view of upper stator

(b) Upper view of lower stator

(c) Cross section view

Fig. 2 The coordinate system.

and the axial force and tilting torques when the rotor is at the equilibrium position become

$$f_z = \sum_{k=1}^{6}(-f_{u,k} + f_{l,k}) \approx \frac{2\mu_0 A_p N H_c t_p}{(2g_0 + t_c + t_p)^2} i_z + \frac{4\mu_0 A_p (H_c t_p)^2}{(2g_0 + t_c + t_p)^3} z \tag{7}$$

$$\tau_x = \sum_{k=1}^{6} r_p\,(-f_{u,k} + f_{l,k}) \sin\frac{(2k-1)\pi}{6} \approx \frac{\mu_0 A_p N H_c t_p r_p}{(2g_0 + t_c + t_p)^2} i_{\theta x} + \frac{2\mu_0 A_p (H_c t_p r_p)^2)}{2g_0 + t_c + t_p)^3} \theta_x \tag{8}$$

$$\tau_y = \sum_{k=1}^{6} r_p\,(f_{uk} - f_{lk}) \cos\frac{(2k-1)\pi}{6} \approx \frac{\mu_0 A_p N H_c t_p r_p}{(2g_0 + t_c + t_p)^2} i_{\theta y} + \frac{2\mu_0 A_p (H_c t_p r_p)^2)}{2g_0 + t_c + t_p)^3} \theta_y \tag{9}$$

Lorentz forces by the coil currents are calculated as

$$f_{L,x,s,k} = l_c B_b i_{s,k} \left(\sin\frac{(k-1)\pi}{3} - \sin\frac{k\pi}{3} \right) \tag{10}$$

$$f_{L,y,s,k} = l_c B_b i_{s,k} \left(-\cos\frac{(k-1)\pi}{3} + \cos\frac{k\pi}{3} \right) \tag{11}$$

Then the radial forces become

$$f_x = \sum_{k=1}^{6} (f_{L,x,u,k} + f_{L,x,l,k}) \approx \frac{6\mu_0 H_c t_p l_c}{2g_0 + t_c + t_p} i_x \tag{12}$$

$$f_y = \sum_{k=1}^{6} \left(f_{L,y,u,k} + f_{L,y,l,k} \right) \approx \frac{6\mu_0 H_c t_p l_c}{2g_0 + t_c + t_p} i_y \tag{13}$$

The analytical results show that the suspension force and torque can be controlled independently.

3. Experimental verification

3.1. Experimental device

A prototype was built to verify the feasibility of the proposed AMB. The photographs are shown in Fig. 3. One side of the rotor consists of a back iron, a cylindrical path (OD:ϕ52 mm, ID:ϕ48 mm), and a PM ring (neodymium magnet N35,

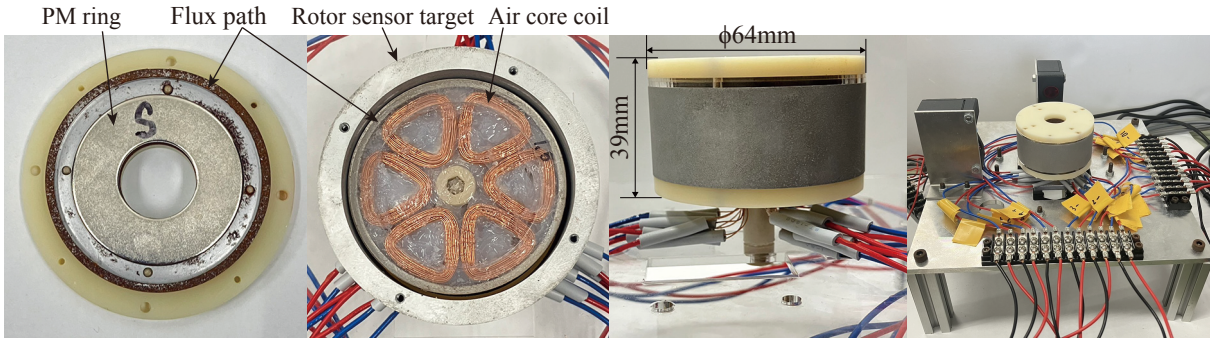

(a) Rotor (b) Stator (c) Side view (d) External view

Fig. 3 Experimental device.

OD:ϕ40 mm, ID:ϕ18 mm, t2 mm). The upper and lower rotors are connected by an outer cylinder. The outer cylinder is also used as sensor target.

The stator contains twelve air-core coils in total, with six located at the top and six at the bottom. Each coil is 68 turns of ϕ3.2 mm polyurethane-coated copper wire. The size of the coils matches to the outer and inner diameters of the PM ring. A drive circuit using a power op-amp (TI OPA548T) supplies current to each coil.

Five laser displacement sensors (OMRON ZX-LD30V) are installed to measure the position of the rotor. tThree sensors measure axial displacement and tilt angles and two sensors measure radial displacement.

The controller is implemented on a digital signal processor (DSP, dSPACE MicroLabBox). The DSP reads the displacement signals via A/D converters, and transforms them into displacement and tilting angles about the center of gravity (COG) of the rotor. The following PD controllers are used for the position control.

$$G_{PD} = K_P + K_D \frac{N}{1 + NT_s \frac{1}{z-1}} \tag{14}$$

where K_P is a proportional gain, K_D is a differential gain, T_s is a sampling time (0.1 ms), N is a filter coefficient of a differentiator (100). The gains were tuned experimentally as shown in Table I. The current in each coil is calculated according to Eqs. (4) and (5), and the current commands are output to the power amplifiers via D/A converters.

Table 1 Parameters of the controller

	z	θ_x	θ_y	x	y
K_P	8.7 A/mm	200 A/deg	200 A/deg	0.15 A/mm	0.15 A/mm
K_D	0.08 As/mm	1.5 As/deg	1.5 As/deg	0.01 As/mm	0.01 As/mm

3.2. Levitation test

Levitation tests were conducted, confirming stable levitation. Figure 4 shows the start-up response. The displacement and tilt angle settled to zero within 0.2 seconds, confirming the feasibility of the proposed AMB. The coil currents were converged to approximately about 0.5 A, and this can be reduced to zero by adjusting the reference levitation position or using zero-power controller.

Figure 5 shows the disturbance response. The disturbance was added manually. It has been confirmed that even when a large external disturbance is applied and the floating position significantly deviates from the equilibrium point, it quickly converges to the equilibrium point.

4. Conclusion

In this paper, we propose a novel five-axis active magnetic bearing and confirm its feasibility through experimental verification. In the future, we plan to clarify the characteristics of the suspension force and investigate rotational loss.

Acknowledgement

This work was supported by JSPS KAKENHI Grant Number 23K03737.

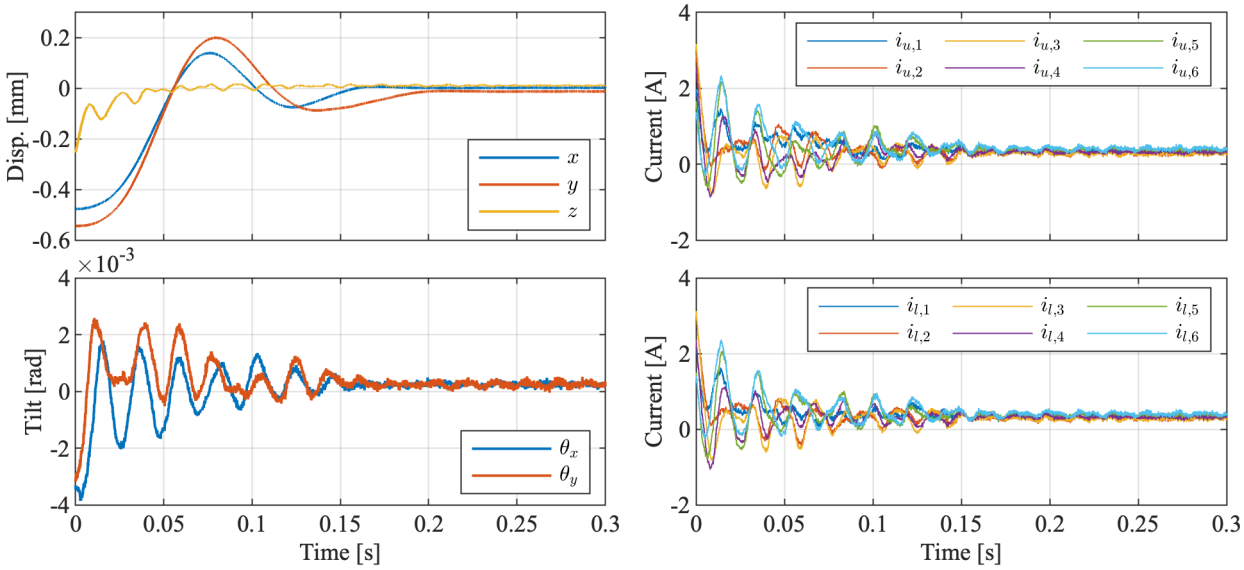

Fig. 4 Start-up response.

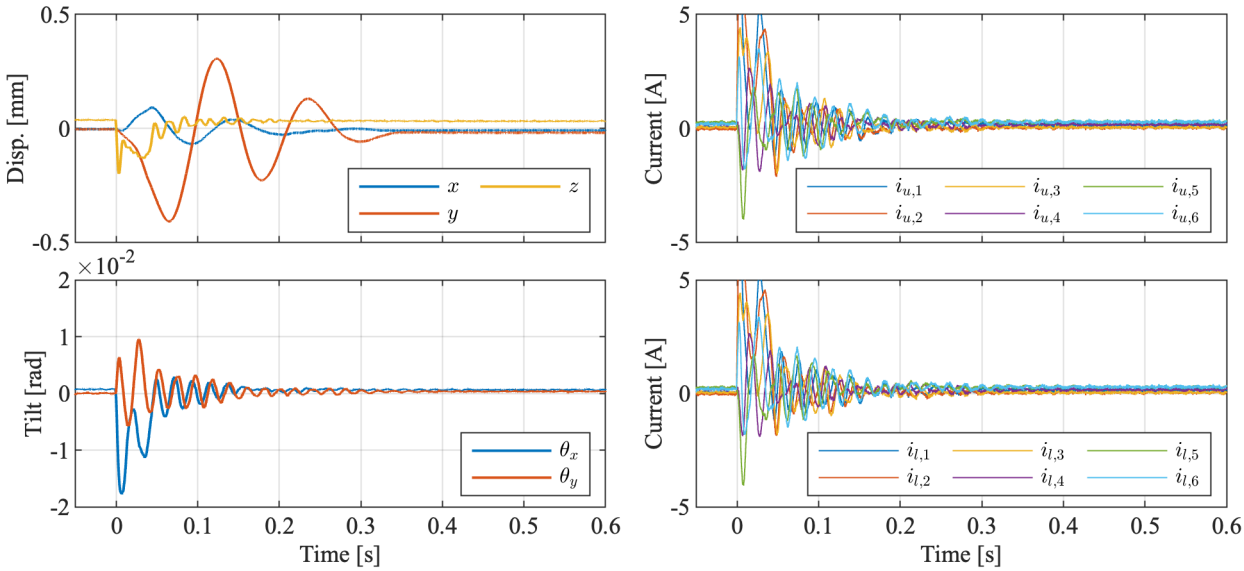

Fig. 5 Disturbance response.

References

Chen, S. L., and Lin, S. Y. , Adaptive imbalance compensation for a three-pole AMB system, 12th IEEE International Conference on Control and Automation (ICCA), Kathmandu, Nepal (2016), pp. 962-965, doi: 10.1109/ICCA.2016.7505404.

Mahmoud S. M., Ueno, S., Jiang C., Power reduction and resonance avoidance of Maglev vertical axis wind turbines using attractive type passive magnetic bearings, Mechanical Engineering Journal, Vol. 7, No. 5 (2020), p. 20-00043.

Matsuzaki T., Takemoto, M., Ogasawara, S., Ota, S. , Oi, K., and Matsuhashi, D., "Novel Structure of Three-Axis Active-Control-Type Magnetic Bearing for Reducing Rotor Iron Loss," in IEEE Transactions on Magnetics, Vol. 52, No. 7 (2016), pp. 1-4, Art no. 8105404, doi: 10.1109/TMAG.2016.2514604.

Nakajima, A., Hirata, K., Niguchi, N., and Kato, M.. "Dynamic characteristics of triaxial active control magnetic bearing with asymmetric structure" Open Physics, Vol. 16, No. 1 (2018), pp. 9-13. https://doi.org/10.1515/phys-2018-0002.

Ueno, S., Inoue, R., Mamada, K., Zhao, C., "Development of Five-Axis Active Controlled Axial-Flux Self-Bearing Motor using Unipolar Magnetic Field", Journal of the Japan Society of Applied Electromagnetics, Vo. 20, No. 2 (2022), pp. 79–85 (in Japanese).